SIMULATION OF A ROOFTOP PHOTOVOLTAIC SYSTEM: A FOCUS ON THE ENERGY PERFORMANCE OF THE BUILDING

Thomas Villemin, Alex Royer, Olivier Farges, Gilles Parent, Remy Claverie

Proceedings of the 17th International Heat Transfer Conference, IHTC-17
14 18 August 2023, Cape Town, South Africa

IHTC-17 | ID: 321

SIMULATION OF A ROOFTOP PHOTOVOLTAIC SYSTEM: A FOCUS ON THE ENERGY PERFORMANCE OF THE BUILDING

Thomas Villemin[1*], **Alex Royer** [1], **Olivier Farges** [1], **Gilles Parent** [1], **Rémy Claverie** [2]

[1]Université de Lorraine, CNRS, LEMTA, F-54000 Nancy, France
[2]Cerema Est, TEAM Research Group, 71 rue de la grande haie F-54510 Tomblaine, France

ABSTRACT

Building Applied Photovoltaics and Building Integrated Photovoltaic systems are promising opportunities to develop renewable technologies in urban environment. However, the photovoltaic field acts as a solar and aeraulic mask for the underlying building that impacts the building's energy needs for air conditioning and heating. In this work, the energy balance of a simplified building with integrated photovoltaic field is modelled using a Monte Carlo approach. This method is applied to evaluate the needs for cooling or heating of the building for several years. Two kinds of roof decks are studied: concrete roof with a single layer and green roof with two additional layers (substrate and vegetation layers). The results from the Monte Carlo simulation are discussed and exploited with a FeedForward Artificial Neural Network to interpolate the building consumption according to the meteorological parameters.

KEY WORDS: Rooftop Photovoltaic systems, Monte Carlo method, Artificial neural network, Multivariate interpolation

1. INTRODUCTION

In recent decades, energy needs have increased significantly and the exploitation of solar energy through photovoltaic panels (PV panels) is particularly interesting. In 2021, the cumulative installed solar capacity worldwide was approximately 843 GW [1]. In urban areas, the installation of PV panels on building roofs is generally favoured because they are very well exposed to solar radiation and urban space can be saved. According to [2], exploitation of rooftops in European Union could produce up to 680 TWh of electricity per year that represents 24.4 % of EU's annual electricity consumption. Moreover, the problem of energy consumption of buildings is also a major issue in urban environments [3]. Thus, in recent years, the installation of combined systems, Building Applied Photovoltaics (BAPV) and Building Integrated PV (BIPV), has intensified [4]. However, the radiative and aeraulic mask effects created by such a PV field will disturb the energy balance of the underlying building and therefore its energy consumption, especially for heating and cooling. The findings are variable depending on the type of climate where the building is located [5, 6, 7]. The general observation is that PV modules lead to a reduction in cooling demand in hot periods and an increase in energy demand in cold periods due to the shading effect created by the PV field. Nevertheless, it is important to perform simulations to validate these statements for different configurations.
In the present study, the energy balance of a simplified building with integrated rooftop PV field is modelled using Monte Carlo approaches [8]. This method has proven to be a successful approach to urban issues and has many advantages: renewed physical images, insensitivity of computation times to the dimension of the integration domain and to the number of coupled phenomena, insensitivity to the geometrical complexity at temporal and spatial scales [9, 10, 11]. The objective of the model is to estimate the building's energy demand for cooling and heating to maintain a target temperature for the air inside the building. Then, the building's

*Corresponding Author: thomas.villemin@univ-lorraine.fr

Table 1: Thermal properties of the green roof structure.

Thermal parameters	Vegetation layer	Substrate layer	Concrete layer
λ $(W \cdot m^{-1} \cdot K^{-1})$	0.3	1	1
ρ $(kg \cdot m^{-3})$	582	1200	1700
C_p $(J \cdot kg^{-1} \cdot K^{-1})$	4800	840	840
Thickness (m)	0.06	0.1	0.15

energy needs are found by the integration of the power over time using double randomization technique [12, 13]. Two configurations are analyzed: (i) the roof is a classic concrete slab, (ii) the concrete slab is overhung by an extensive green roof with substrate and vegetation layers. The simulations are conducted for different locations in the world using Typical Meteorological Year (TMY) data for weather parameters (solar irradiation, air temperature and wind speed): Reykjavik (Iceland), Las Vegas (USA), Cape Town (South Africa), Melbourne (Australia), Nancy (France).
Finally, a Feedforward Artificial Neural Network (FANN) is implemented to exploit the information obtained from the Monte Carlo random paths. For each path, the estimated power and the meteorological parameters are stored, then used to train a neural network. Time evolution of the total power for heating and cooling of the building is obtained by a multivariate regression function implicitly determined by the trained neural network according to the meteorological parameters. As a final step, the energy is calculated by time integration of the power. The results obtained by the neural network are compared with the simulation points obtained by the Monte Carlo method.

2. STUDIED CONFIGURATION

The studied geometry is a simplified building with a flat roof. The height of the building is 3 m, the base is square and 10 m long inside the building. The thickness of the walls is set at 0.2 m. The walls and the floor are supposed to be made of concrete. For the roof two cases are studied, the first one with only a concrete roof (fig. 1a) and the second one with three layers (fig. 1b). The two additional layers correspond to a situation where an extensive green roof is installed on the building. The top layer represents a vegetation layer and the middle one is the substrate layer where the plants take root. The thermal conductivities, material densities and heat capacities of the different layers of green roof are provided in table 1. Moreover, the building is studied for two different rooftop configurations: (i) without PV field, (ii) with rooftop PV field.

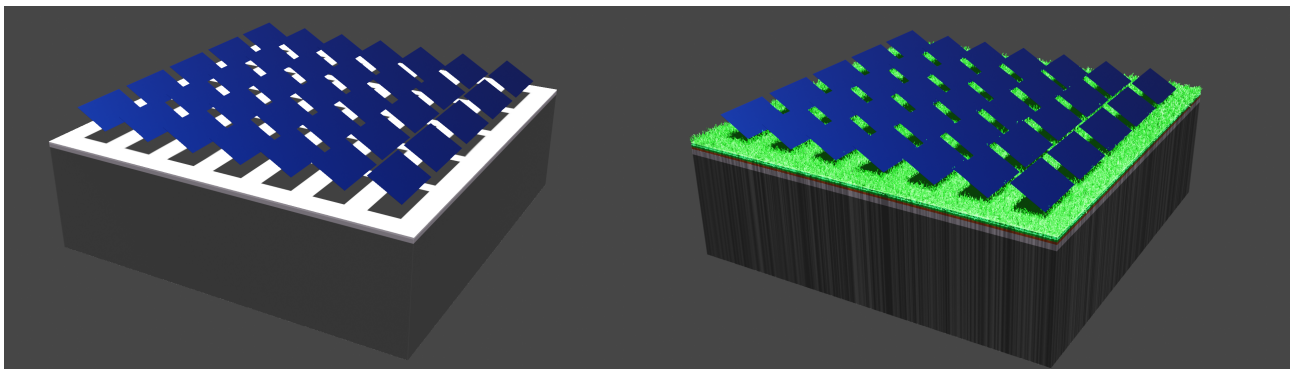

(a) Building geometry with concrete configuration. **(b)** Building geometry with green roof configuration.

Fig. 1: Building geometry and rooftop photovoltaic field.

When present, the photovoltaic field almost entirely covers the roof and the PV field acts as a solar mask and aeraulic obstacle for the underlying building. This selected situation should provide insights about how the energy requirements of a building change with the presence or the absence of a rooftop PV field.

The temperature at the bottom of the ground is set at 17 °C[1]. The target temperature for the air inside the building is 19 °C. For convective heat transfer between indoor air and indoor walls, the convective heat transfer coefficient is set at $10\,\mathrm{W}\cdot\mathrm{m}^{-2}$. For outside convective heat transfer coefficient, the formula from MacAdams [14] is used.
The dimensions of the PV panels are quite standard with a length of 1.6 m and width of 1 m. The distance between the bottom of the PV panels and the top of the roof is set at 0.5 m which is rather usual for rooftop mounting configuration. The PV panels are facing south direction and the tilt angle is 30°. The PV field is composed of 7 rows of 5 panels each, for a total of 35 panels.

3. METHODS

In the present work, the Monte Carlo statistical method is used to evaluate physical quantities of interest at a probe point and a feedforward artificial neural network is used as a nonlinear multivariate interpolator based on data obtained with Monte Carlo simulations. The proposed model, based on the Monte Carlo method, has many advantages including the handling of the 3D geometric complexity of the building and its environment. Moreover, the Monte-Carlo method has already proven its ability to handle complex geometries [8] as well as to take into account transient phenomena with high variability as solar energy. [15].

3.1. Monte Carlo modelling of heat transfer In this framework, the physical quantity is expressed as the expectation of a random variable. In the context of this paper, the physical quantity is the heating or cooling energy requirement of the building to maintain a given air temperature. The total energy needs are computed from the integration over time of the power $P(t)$ (see eq. (1)), both for cooling and heat requirements. The power to be supplied to the building to meet its energy needs is calculated as the power exchanged between the wall temperature ($T_w(\mathbf{x},t)$) and T_{cooling} (respectively T_{heating}) for the cooling (respectively heating) requirement.

$$P(t) = \mathbb{E}[\mathscr{P}(t)] = \int_{\partial S} \mathrm{d}S\, p_{\mathbf{X}}(\mathbf{x}) \left[h_{\text{cv}}^{\text{in}} \left[(T_{\text{heating}} - T_w(\mathbf{x},t))\mathscr{H}(T_w(\mathbf{x},t) < T_{\text{heating}}) + (T_w(\mathbf{x},t) - T_{\text{cooling}})\mathscr{H}(T_w(\mathbf{x},t) > T_{\text{cooling}})\right]\right] \tag{1}$$

where T_{heating} is the temperature below which heat must be supplied to the building, T_{cooling} is the limit temperature at which it is considered necessary to have air-conditioning, $T_w(\mathbf{x},t)$ is the temperature of the wall of the room, $p_{\mathbf{X}}$ is the density probability function to sample a position on a wall inside the room (chosen uniformly in this work), $h_{\text{cv}}^{\text{in}}$ is the indoor convective coefficient and $\mathscr{H}(x)$ is the Heaviside step function. $T_w(\mathbf{x},t)$ is also expressed as the expectation of a random variable $\Theta(\mathbf{x},t)$ and thanks to double randomization [12, 13], the quantities $P(t)$ and E_{total} (see eq. (2)) can be obtained using a single Monte Carlo algorithm. The Monte Carlo algorithm for the evaluation of $T_w(\mathbf{x},t)$ is described in alg. 1 and the corresponding figure is shown in fig. 2 where conductive, convective and radiative heat transfers have a statistical description.

$$E_{\text{total}} = \mathbb{E}[\mathscr{E}] = \int_{t_I}^{t_F} \mathrm{d}\tau\, p_\tau(\tau)\mathscr{P}(\tau) \tag{2}$$

where t_I and t_F are the initial and final times, p_τ is the density probability function to sample the time over the interval $[t_I, t_F]$ (this function is chosen uniformly in this work) and $\mathscr{P}(\tau)$ is the power for cooling and heating requirements.
To estimate $T_w(\mathbf{x},t)$, a path starts at a random position $\mathbf{x}$ on one of the walls of the room (including roof and ground surfaces) at a given time. Then the path goes backward in time until the initial or a known temperature is reached. It has to be noted that walls of the building are not considered isothermal. The Monte Carlo algorithm accounts for fully coupled heat transfers in the building, including conduction in the wall, convection and radiation which occur at the surfaces. For the transient conductive heat transfer inside the solid domains, diffusive random walks are used. At each step of the random walk in conduction, the current time is decreased of a quantity depending on the material thermal inertia. When surfaces of the solid domain are encountered, the

[1] Strictly speaking, this temperature should depend on the location of the building and the depth in the ground, this could be discussed further. As this temperature is not a major issue in this work, it is set at 17 °C regardless of the geographical location studied.

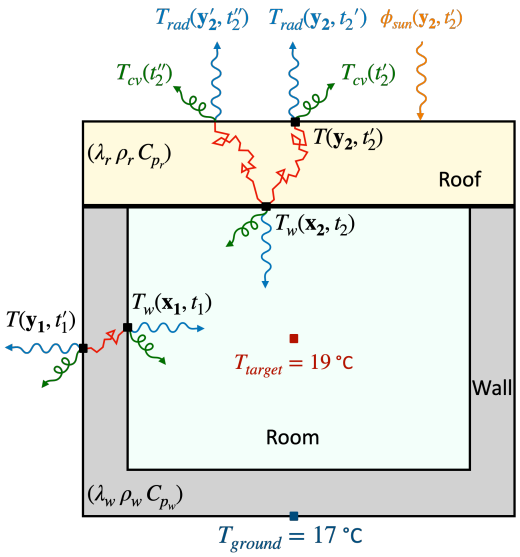

Fig. 2: Building geometry and conducto-convective-radiative transfers at interfaces

flux continuity equation is written and the path couples conductive, convective and radiative heat transfers as written in eq. (3). Only for these interfaces with the outdoor environment, the meteorological data are needed (air temperature, solar irradiation, wind speed). For solar irradiation, depending on the position of the sun and the shading effect created by the photovoltaic field, its contribution to the wall temperature can be zero.

$$T(\mathbf{y},t) = \mathbb{P}_{\text{cd}\to\text{cd}} T(\mathbf{y}-\delta_r\mathbf{n},t) + \mathbb{P}_{\text{cd}\to\text{cv}} T_{\text{air}}(t) + \mathbb{P}_{\text{cd}\to\text{rad}} \int_{2\pi} \mathrm{d}\omega\, p_\Omega(\omega) T_{\text{rad},-\omega}(\mathbf{y},t) + \frac{1}{\lambda/\delta + h_{\text{cv}} + h_{\text{rad}}} \int_{2\pi} \mathrm{d}\omega\, p_\Omega(\omega) |\omega\cdot\mathbf{n}| \mathscr{H}(\mathbf{Y}\notin \text{PV}) \phi_{\text{sun}}(\mathbf{y},t) \quad (3)$$

In eq. (3), $\mathbf{n}$ is the normal vector at the interface oriented towards the outside, $\mathbb{P}_{\text{cd}\to\text{cd}} = \frac{\lambda/\delta}{\lambda/\delta+h_{\text{cv}}+h_{\text{rad}}}$, $\mathbb{P}_{\text{cd}\to\text{cv}} = \frac{h_{\text{cv}}}{\lambda/\delta+h_{\text{cv}}+h_{\text{rad}}}$ and $\mathbb{P}_{\text{cd}\to\text{rad}} = \frac{h_{\text{rad}}}{\lambda/\delta+h_{\text{cv}}+h_{\text{rad}}}$ are probabilities depending on material properties and thermal exchange coefficients and δ the moving step for the random walk in the solid domain. The solar flux is taken into account when the sampled ray in the direction ω does not intercept the photovoltaic field (for the roof surface) and when the sun is facing the building's surface for the other walls. p_Ω is the density probability to sample a unit hemisphere at the surface.

3.2. FANN interpolation Based on the results of the Monte Carlo calculations, we aim to develop a tool that can quickly and accurately estimate the required heating or cooling capacity according to meteorological parameters over a typical year. A feedforward artificial neural network (FANN) is used and trained on a database built from the probe point calculations of the stochastic algorithm described above. It is used as a nonlinear multivariate interpolator. It has been shown that this type of network is capable of modelling any continuous function over a given interval [16, 17]. The neural network, in the same way as a more classical correlation, is then comparable to a reduced model of the treated problem which depends on many independent parameters. The network is composed of elementary computing units (see fig. 3a) interconnected and organized in successive layers (see fig. 3b). In this work, we will use ANN with only one hidden layer.
The output of each neuron can be calculated as follows:

$$a = \sigma\left(\sum_j \omega_j x_j + b\right) = \sigma(z) \quad (4)$$

Where σ is the activation function of the neuron, ω_i and x_i are respectively the i^{th} weight and input and b the bias. For regression tasks, functions of the sigmoid family are classically used. In the present study, the

Algorithm 1: Monte Carlo algorithm to estimate the temperature $T_w(\mathbf{x},t)$.

Sample a wall and a position $\mathbf{x_1}$ to estimate $T_w(\mathbf{x_1},t_1)$
$\mathbf{x} = \mathbf{x_1}$
$t = t_1$
$w = 0$
$A = 0$ (accumulation term to account for solar irradiance)
while $t > t_I$ **do**
    Sample τ according to exponential law according to the material properties λ, ρ, C_p
    $t = t - \tau$
    if $t < t_I$ **then**
        $w = w + T_I(\mathbf{x}) + A$
    else
        if $\mathbf{x} == \mathbf{x_1}$ *or* $\mathbf{x} == \mathbf{y_1}$ **then**
            Calculate $\mathbb{P}_{\text{cd}\to\text{cd}}$ and $\mathbb{P}_{\text{cd}\to\text{cv}}$ according to the continuity equation (eq. (3))
            Sample r according to uniform law between 0 and 1
            if $r < \mathbb{P}_{cd\to cd}$ **then**
                $\mathbf{x_1} = \mathbf{x_1} + \delta\mathbf{n}$ (random walk continues into conduction in the solid)
            else if $r < \mathbb{P}_{cd\to cd} + \mathbb{P}_{cd\to cv}$ **then**
                Evaluate A for solar irradiance contribution according to eq. (3)
                $w = w + T_{\text{cv}}(t) + A$
            else
                Evaluate A for solar irradiance contribution according to eq. (3)
                $w = w + T_{\text{rad}}(\mathbf{x},t) + A$
            end
        else
            Conduction in the solid domain using a random walk on δ-sphere
        end
    end
end

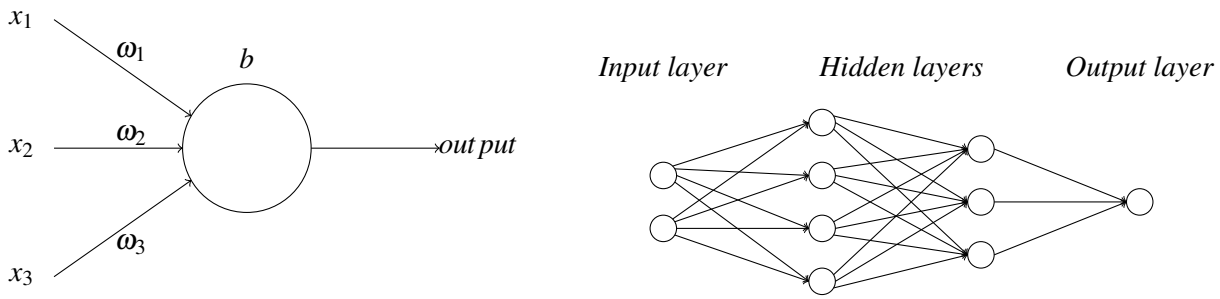

(a) Simple neuron representation.

(b) Diagram of a two layer neural network.

Fig. 3: Neuron representation and two layer neural network.

hyperbolic tangent is implemented. The network used consists of only one hidden layer of 25 neurons.
To train the neural network, we use a Levenberg Marquardt algorithm [18] combined with Bayesian regularisation [19, 20]. This method is known to converge particularly quickly but requires the calculation of the Hessian matrix for the database used. Therefore, it is relatively computationally intensive compared to other methods and that limits the size of the database that can be used. Bayesian regularisation is used to *guide* the learning process and to penalise network weights ω_j that are too high. If we do not use regularisation, the cost function,

here the MSE, can be expressed as follows:

$$C = E_d = \frac{1}{2N}\sum_i [t(i) - a(i)]^2 \tag{5}$$

Where, N is the number of training set, $t(i)$ the i^{th} theoretical output (from the database) and $a(i)$, the i^{th} response of the ANN. With the bayesian regularisation, we have :

$$C = \alpha E_d + \beta E_w \tag{6}$$

Where E_W is the sum of squares of the network weights. The hyperparameters α and β are computed during the algorithm as follows :

$$\alpha = \frac{\gamma}{2E_W} \tag{7}$$

$$\beta = \frac{N_{out} - \gamma}{2E_D} \tag{8}$$

$$\gamma = n - 2\alpha \,\mathrm{Tr}\left\{He^{-1}\right\} \tag{9}$$

With n is the total number of parameters and N_{out}, the number of training output data. In these equations, γ is the effective number of parameters. This quantity is also calculated during the algorithm thanks to the Bayesian paradigm and gives us information on the number of parameters useful for modelling the target function. In other words, this coefficient informs us about the relevance of the topology used and implicitly, about the number of neurons on the hidden layer. The value of γ is calculated according to the trace of the Hessian matrix $\mathrm{Tr}\left\{He^{-1}\right\}$ and is thus adapted to the database used. The α and β coefficients are also modified during the training according to the database in an optimal way. These characteristics mean that this method has particularly powerful generalisation capabilities and is very little sensitive to overfitting. Finally, in the theoretical development of Bayesian regularisation, it is assumed that the theoretical responses from the database are subject to Gaussian error. Although this assumption is not generally correct, the Monte Carlo algorithm used to generate the training data implies by construction this type of numerical error. This training method is therefore particularly suitable for the case under study. This methodology, combining a monte carlo algorithm and Bayesian regularisation, has already been successfully used to calculate the field thermal radiation in aeronautical combustion chambers [21].
We can summarise the whole algorithm used here by the following procedure:

Algorithm 2: FAAN

```
1  Training data normalization
2  Random initialization of the parameters
3  while Nb_epoch < criterion do
4      foreach training set of the batch do
5          Feedforward pass:
6              Compute the individual network output, the associated error and the sensivity vector δ^L
7              on the last layer
8          Backward pass:
9              Retropropagation of the sensitivities δ^l in each layer l
10         Calculation of the Jacobien and Hessian matrices
11     end
12     foreach Parameter in each layer l do
13         Update the weights and the biases
14         Update the hyperparameters α, β and γ
15     end
16     Repeat the procedure between points 3 and 4 for each epoch until a stopping criterion is reached
17 end
```

The maximal number of epochs is set at 1000. The data set was normalised before training between -1 and 1 depending on the minimum and maximum of each parameter. To train the neural network, we use a code developed in C language and based on the algorithms described in [18]. The training of the neural networks

is conducted on a four cores standard desktop computer equipped with an Intel Core i5-8265U processor and 15.5 GB of RAM.

4. RESULTS

Weather data are extracted from the National Solar Radiation Database (NSRDB[2]) from the NREL laboratory and from the Photovoltaic Geographical Information System (PVGIS[3]). The global horizontal irradiance ($W \cdot m^{-2}$), the wind speed ($m \cdot s^{-1}$) and the air temperature (°C) are available at hourly time step. The solar elevation (°) and the solar azimuth (°) angles are calculated using the Python's tool pvlib[4]. The three main weather data are plotted for the cities of Las Vegas, Nancy and Cape Town in fig. 4.

Fig. 4: Weather data (global horizontal irradiance, air temperature and wind speed) for 2019 for Las Vegas, Cape Town and Nancy. For the radiation data the daily maximum is displayed and for the air temperature the daily average is plotted.

The total power for the building needs is estimated using the Monte Carlo algorithm for random times during the 2019 year. Then the Feedforward Artificial Neural Network is used to interpolate these points to simulate the power over a summer week for Las Vegas and Cape Town. The two selected weeks correspond to a summer and a winter season for both cities. The neural network was also tested with a training using only TMY data instead of 2019 data to estimate the power for the 2019 year. The obtained results demonstrate the robustness of the FANN to predict the power simulated with the Monte Carlo method and are shown in **??** and fig. 5 for the concrete rooftop configuration (one layer only) with and without photovoltaic field for the summer week. The result for the green roof configuration is given in fig. 6 for Las Vegas during the summer week and demonstrates similar behaviour for this rooftop configuration.
The database used to train the neural network consists of 6500 parameter sets from 5 different cities in both PV and non-PV configurations. In other words, on average, the neural network only *saw* less than 2 points per day per configuration during training to be able to interpolate with as much accuracy the power needed for heating or cooling at each moment of the year 2019. In fig. 5 and **??**, the network was trained on an average year and therefore different from the one on which it interpolated its results. Under these conditions, the integration of

[2] https://nsrdb.nrel.gov/
[3] https://re.jrc.ec.europa.eu/pvg_tools/en/
[4] https://pvlib-python.readthedocs.io/en/stable/

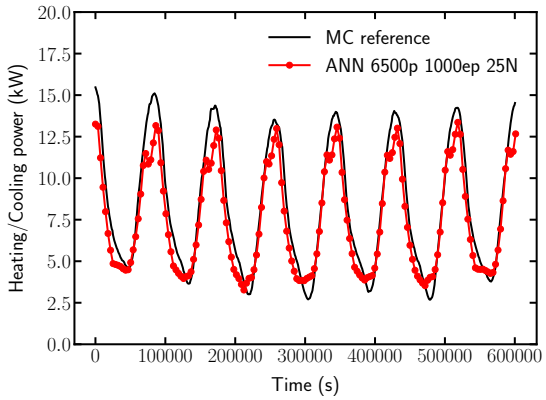

(a) Las Vegas, 2019 Summer week: Monte Carlo simulation in black color (reference solution), interpolation using TMY with the FANN in red color. Configuration with photovoltaic field and concrete roof.

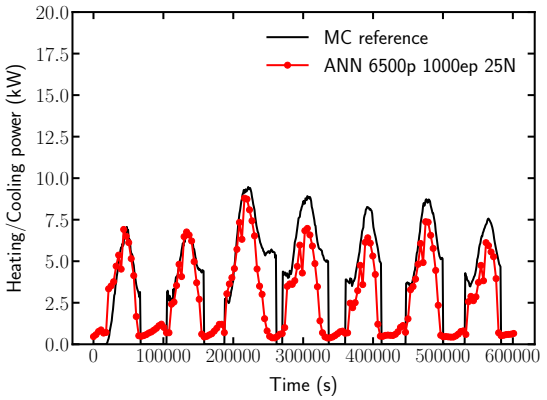

(b) Cape Town, 2019 Summer week: Monte Carlo simulation in black color (reference solution), interpolation using TMY with the FANN in red color. Configuration with photovoltaic field and concrete roof.

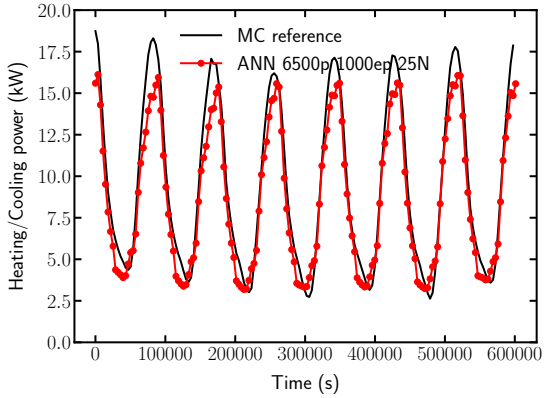

(c) Las Vegas, 2019 Summer week: Monte Carlo simulation in black color (reference solution), interpolation using TMY with the FANN in red color. Configuration without photovoltaic field and concrete roof.

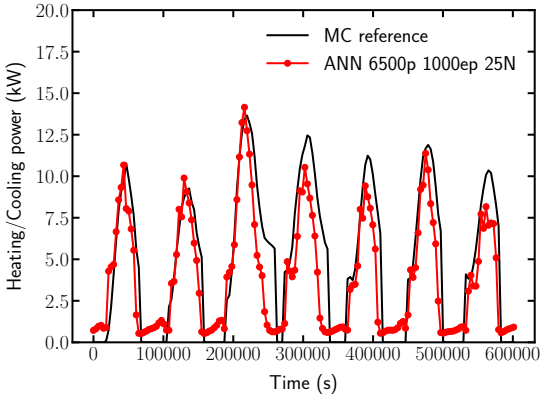

(d) Cape Town, 2019 Summer week: Monte Carlo simulation in black color (reference solution), interpolation using TMY with the FANN in red color. Configuration without photovoltaic field and concrete roof.

Fig. 5: Monte Carlo simulation points and FANN interpolation for Las Vegas and Cape Town in 2019 summer periods for the concrete roof configuration, with and without photovoltaic field.

Table 2: Energy evaluation of the building's energy needs for the concrete configuration without photovoltaic field in 2019 and comparison between the Monte Carlo algorithm (10^6 realizations) and the FANN.

City		Monte Carlo		FANN	
		Energy (MWh) $\pm\sigma$	Comp. time (s)	Energy (MWh)	Comp. time[5](s)
Las Vegas	No PV	53.04 $\pm$0.23	10.192	50.43	$74 \cdot 10^{-6}$
	PV	45.04 $\pm$0.19	10.260	43.76	$74 \cdot 10^{-6}$
Cape Town	No PV	26.95 $\pm$0.22	9.717	25.75	$65 \cdot 10^{-6}$
	PV	20.70 $\pm$0.20	9.599	19.61	$63 \cdot 10^{-6}$

[5] Interpolation time for 8760 points over the whole year (every hour) and for numerical integration.

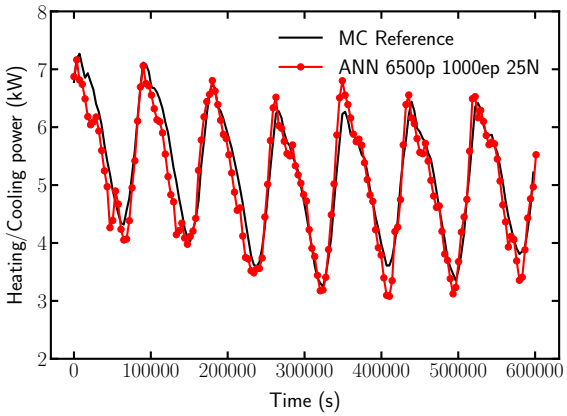

Fig. 6: Las Vegas, 2019 Summer week: Monte Carlo simulation in black color (reference solution), interpolation using TMY with the FANN in red color. Configuration with photovoltaic field, green roof layer.

the power calculated by the network over the whole year makes it possible to calculate an energy requirement that is very close, to within a few percent, to that obtained by the Monte Carlo method. This flexibility and this robustness demonstrate the great capabilities of this type of tool for the development of accurate and efficient scale models. Results for winter periods are not presented here but our simulations suggest that the presence of the photovoltaic field is advantageous in reducing the needs of the building. In the same way, in the summer period, it seems that the air conditioning consumption is higher without the photovoltaic field.

5. CONCLUSIONS

The results show that the energy required to heat and cool the building is lower for a rooftop PV configuration for Las Vegas and Cape Town in 2019 with a difference of 8 MWh for Las Vegas and 6 MWh for Cape Town. Moreover, the configuration with a green roof tends to favour this effect with an additional thermal insulation brought by the two additional layers (vegetation and substrate layers). Finally, the neural network interpolation, using the FANN model, proved to be particularly efficient with only 6500 training Monte Carlo points for all 5 cities studied and the configurations with and without photovoltaic panels. In a future work, it is envisaged to conduct a sensitivity study on the building parameters: number of layers, thermal properties etc.

ACKNOWLEDGEMENT

This research work was carried out within the scope of the PROOF Project, funded by the French National Research Agency (ANR) under the grant number no ANR-19-CE22-008.

REFERENCES

[1] Irena. https://irena.org/solar.

[2] Katalin Bódis, Ioannis Kougias, Arnulf Jäger-Waldau, Nigel Taylor, and Sándor Szabó. A high-resolution geospatial assessment of the rooftop solar photovoltaic potential in the european union. *Renewable and Sustainable Energy Reviews*, 114:109309, 2019.

[3] Ziwei Li, Borong Lin, Shanwen Zheng, Yanchen Liu, Zhe Wang, and Jian Dai. A review of operational energy consumption calculation method for urban buildings. *Building Simulation*, 13(4):739–751, 2020.

[4] Aritra Ghosh. Potential of building integrated and attached/applied photovoltaic (bipv/bapv) for adaptive less energy-hungry buildings skin: A comprehensive review. *Journal of Cleaner Production*, 276:123343, 2020.

[5] Yue Wang, Dengjia Wang, and Yanfeng Liu. Study on comprehensive energy-saving of shading and photovoltaics of roof added pv module. *Energy Procedia*, 132:598–603, 2017. 11th Nordic Symposium on Building Physics, NSB2017, 11-14 June 2017, Trondheim, Norway.

[6] Yawar Ali Sheikh, Muhammad Umar Maqbool, Arslan Dawood Butt, Abdul Rauf Bhatti, Ahmed Bilal Awan, Kashif Nisar Paracha, and Muhammad Murad Khan. Impact of rooftop photovoltaic on energy demand of a building in a hot semi-arid climate. *Journal of Renewable and Sustainable Energy*, 13(6):065101, 2021.

[7] Habeeb Alasadi, Jun-Ki Choi, and Rydge B Mulford. Influence of photovoltaic shading on rooftop heat transfer, building energy loads, and photovoltaic power output. *Journal of Solar Energy Engineering*, 144(6):061011, 2022.

[8] Morgan Sans, Olivier Farges, Vincent Schick, and Gilles Parent. Solving transient coupled conductive and radiative transfers in porous media with a monte carlo method: Characterization of thermal conductivity of foams using a numerical flash method. *International Journal of Thermal Sciences*, 179:107656, 2022.

[9] Najda Villefranque, Frédéric Hourdin, Louis d'Alençon, Stéphane Blanco, Olivier Boucher, Cyril Caliot, Christophe Coustet, Jérémi Dauchet, Mouna El Hafi, Olivier Farges, et al. The" teapot in a city": a paradigm shift in urban climate modeling. *arXiv preprint arXiv:2204.14227*, 2022.

[10] Loris Ibarrart, Stéphane Blanco, Cyril Caliot, et al. Advection, diffusion and linear transport in a single path-sampling monte-carlo algorithm: getting insensitive to geometrical refinement. *https://hal.science/hal-03818899*, 2022.

[11] Jean-Marc Tregan, Jean-Luc Amestoy, Mégane Bati, et al. Coupling radiative, conductive and convective heat-transfers in a single monte carlo algorithm: a general theoretical framework for linear situations. *https://hal.science/hal-03819157*, 2022.

[12] Sylvain Maire and Giang Nguyen. Stochastic finite differences for elliptic diffusion equations in stratified domains. *Mathematics and Computers in Simulation*, 121:146–165, 2016.

[13] Mireille Bossy, Nicolas Champagnat, Hélène Leman, Sylvain Maire, Laurent Violeau, and Mariette Yvinec. Monte carlo methods for linear and non-linear poisson-boltzmann equation. *ESAIM: Proceedings and Surveys*, 48:420–446, 2015.

[14] W.H. McAdams. *Heat Transmission*. 1954.

[15] Olivier Farges, Jean-Jacques Bézian, Hélène Bru, Mouna El Hafi, Richard Fournier, and Christophe Spiesser. Life-time integration using monte carlo methods when optimizing the design of concentrated solar power plants. *Solar Energy*, 113:57–62, 2015.

[16] Moshe Leshno, Vladimir Ya. Lin, Allan Pinkus, and Shimon Schocken. Multilayer feedforward networks with a nonpolynomial activation function can approximate any function. *Neural Networks*, 6(6):861–867, January 1993.

[17] Kurt Hornik, Maxwell Stinchcombe, and Halbert White. Multilayer feedforward networks are universal approximators. *Neural Networks*, 2(5):359–366, 1989.

[18] M. T. Hagan, H. B. Demuth, M. H. Beale, and O. De Jesus. *Neural Network Design*. 2th edition, 1996.

[19] D Foresee and M. T. Hagan. Gauss-newton approximation to bayesian learning. In *Proceeding of International Conference on Neural Networks, Houston, Texas, USA*, pages 1930–1935. IEEE, 1997.

[20] D. J. C. MacKay. Bayesian interpolation. *Neural Computation*, 4(3):415–447, 1992.

[21] Alex Royer, Olivier Farges, Pascal Boulet, and Daria Burot. A new method for modeling radiative heat transfer based on bayesian artificial neural networks and monte carlo method in participating media. *Int. J. Heat Mass Transf.*, 201:123610, 2023.